The 2014 World Congress on
Advances in Civil, Environmental, and Materials Research (ACEM14)
Busan, Korea, August 24-28, 2014

Bayesian operational modal analysis and uncertainty assessment incorporating multiple setups

YC Ni and *FL Zhang

Research Institute of Structural Engineering and Disaster Reduction, College of Civil Engineering, Tongji University, China
**corresponding author: fengliangzhang@tongji.edu.cn*

ABSTRACT

In full-scale ambient vibration tests, it is often required to obtain a detailed mode shape of a structure with a limited number of sensors. A common method is to perform multiple setups with each one covering different parts of the structure while sharing some reference degrees of freedom (dofs) in common. In this work, a Bayesian statistical framework is developed for modal identification of well-separated modes incorporating ambient vibration data, i.e., operational modal analysis, from multiple setups. The method views modal identification as an inference problem where probability is used as a measure for the relative plausibility of outcomes given a model of the system and measured data. It allows the global mode shape to be determined taking into account the quality of data in different setups. A fast iterative algorithm is developed that allows practical implementation even for a large number of dofs and setups. On the basis of the negative log-likelihood function (NLLF), the posterior uncertainty of the modal parameters in terms of their covariance matrix is investigated. Analytical expressions are derived so that the posterior uncertainty of modal parameters can be evaluated accurately and efficiently without resorting to finite difference. The proposed method is applied to field test data of a footbridge. Some challenges are revealed in operational modal analysis incorporating multiple setups.

1. INTRODUCTION

The response of a structure subjected to dynamic loads is characterized by its modal properties, including the natural frequencies, damping ratios and mode shapes. Ambient vibration tests are frequently used for their economy in implementation (e.g., Peeters and De Roeck, 2001; Brownjohn, 2003; Au and Zhang, 2012). In full-scale ambient tests, many situations exist where there is a large number of degrees of freedom (dofs) to be measured. The number of available sensors is often limited, however. This means that the dofs of interest cannot be measured synchronously in a single setup and multiple setups are needed to cover all dofs. Conventionally the modal properties in different setups are

identified separately using their corresponding data. The overall mode shape is then assembled (or 'glued') from the partial mode shapes in different setups. The dofs measured in different setups need to share some 'reference dofs'. If there is only one reference dof common to all setups then the overall mode shape can be assembled by simply adjusting the scaling of the mode shapes in different setups. The problem becomes nontrivial when there is more than one reference dof, or when no reference dof is shared by all the setups. The former happens frequently because it is more robust to have reference dofs at possibly multiple locations, for fear of some of the reference dofs lacking modal contribution in a particular mode. More complicated situations exist when the reference sensors (or even the console) need to change in some setups (Zhang and Au, 2011). This paper presents a fast Bayesian method for modal identification incorporating data from multiple setups together with the posterior uncertainty of the modal parameters. The method extends the Fast Bayesian FFT algorithm developed previously for a single setup (Au, 2011b). Theoretical and computational issues of the mode shape assembly problem are addressed. A fast computational procedure for practical application is analyzed in order to develop with possibly a large number of dofs. Field testing data are used to illustrate the proposed method.

2. BAYESIAN FORMULATION FOR MULTIPLE SETUPS

Let $\boldsymbol{\varphi} \in R^n$ be the theoretical mode shape covering all the interested dofs, where n is their number. Assume that there are n_s setups, each covering a possibly different set of dofs. To relate the 'global mode shape' $\boldsymbol{\varphi}$ to that in a given setup, define the selection matrix in Setup i $(i = 1,...,n_s)$, $\mathbf{L}_i \in R^{n_i \times n}$, where n_i is the number of measured dofs in Setup i . The (j,k) entry of $\mathbf{L}_i$ is equal to 1 if dof k is measured by the j-th channel in Setup i; and zero otherwise. Then

$$\boldsymbol{\varphi}_i = \mathbf{L}_i \boldsymbol{\varphi} \in R^{n_i} \tag{1}$$

is the theoretical mode shape confined to the measured dofs in Setup i. Since some dofs are measured in more than one setup, in general $n < \sum_{i=1}^{n_s} n_i$. Throughout this work, it is assumed that $\|\boldsymbol{\varphi}\| = (\boldsymbol{\varphi}^T \boldsymbol{\varphi})^{1/2} = 1$. In the spirit of mode shape assembly, the global mode shape $\boldsymbol{\varphi}$ is assumed to be the same in all setups, although in every setup only its observed part, i.e., $\boldsymbol{\varphi}_i = \mathbf{L}_i \boldsymbol{\varphi}$, is influential to the corresponding data. For the remaining modal parameters, each setup is parameterized with separate values, i.e.,

$$\boldsymbol{\theta} = [\, f_i, \zeta_i, S_i, S_{ei} : i = 1,...,n_s; \boldsymbol{\varphi} \in R^n \,] \in R^{4n_s + n} \tag{2}$$

where $f_i, \zeta_i, S_i, S_{ei} (i = 1,...,n_s)$ are the natural frequency, damping ratio, PSD of modal force and PSD of prediction error of Setup i, respectively.

Let $\mathbf{Z}_k^{(i)} = [\mathrm{Re}\mathcal{F}_{ik}; \mathrm{Im}\mathcal{F}_{ik}] \in R^{2n_i} (i = 1,...,n_s)$ be an augmented vector comprising the real and imaginary part of the FFT $\mathcal{F}_{ik}$ of the measured data at frequency f_k in Setup i; $\mathcal{D}_i = \{\mathbf{Z}_k^{(i)}\}$ denote the FFT data of the selected frequency band in Setup i and $\mathcal{D} = \{\mathcal{D}_i : i = 1,...,n_s\}$ denote the collection of all setups. It is assumed that the data in different setups are statistically independent. Together with a uniform prior distribution, the posterior PDF of $\boldsymbol{\theta}$ given the data in all setups is given by, using Baye's Theorem,

$$p(\boldsymbol{\theta} \mid \mathcal{D}) \propto p(\{\mathcal{D}_1, \mathcal{D}_2, ..., \mathcal{D}_{n_s}\} \mid \boldsymbol{\theta}) = p(\mathcal{D}_1 \mid \boldsymbol{\theta}) p(\mathcal{D}_2 \mid \boldsymbol{\theta}) ... p(\mathcal{D}_{n_s} \mid \boldsymbol{\theta}) \tag{3}$$

To analyze each $p(\mathcal{D}_i \mid \boldsymbol{\theta})$, note that it does not depend on the modal parameters of other setups, i.e., $p(\mathcal{D}_i \mid \boldsymbol{\theta}) = p(\mathcal{D}_i \mid f_i, \zeta_i, S_i, S_{ei}, \boldsymbol{\varphi}_i)$. Thus

$$p(\boldsymbol{\theta} \mid \mathcal{D}) \propto \prod_{i=1}^{n_s} p(\mathcal{D}_i \mid f_i, \zeta_i, S_i, S_{ei}, \boldsymbol{\varphi}_i) \tag{4}$$

In terms of the NLLF, this means

$$L(\boldsymbol{\theta}) = \sum_{i=1}^{n_s} L_i(\boldsymbol{\theta}_i) \tag{5}$$

where $\boldsymbol{\theta}_i = \{f_i, \zeta_i, S_i, S_{ei}, \boldsymbol{\varphi}_i\}$ and

$$L_i(\boldsymbol{\theta}_i) = \frac{1}{2} \sum_k [\ln \det \mathbf{C}_{ik}(\boldsymbol{\theta}_i) + \mathbf{Z}_k^{(i)T} \mathbf{C}_{ik}(\boldsymbol{\theta}_i)^{-1} \mathbf{Z}_k^{(i)}] \tag{6}$$

with $\det(.)$ denoting the determinant and

$$\mathbf{C}_{ik}(\boldsymbol{\theta}_i) = \frac{S_i D_{ik}}{2} \begin{bmatrix} \boldsymbol{\varphi}_i \boldsymbol{\varphi}_i^T & 0 \\ 0 & \boldsymbol{\varphi}_i \boldsymbol{\varphi}_i^T \end{bmatrix} + \frac{S_{ei}}{2} \mathbf{I}_{2n_i} \tag{7}$$

being the theoretical covariance matrix of the FFT data at the k-th frequency abscissa in Setup i; $\mathbf{I}_{2n_i} \in R^{2n_i}$ denotes the identity matrix;

$$D_{ik}(f_i, \zeta_i) = [(\beta_{ik}^2 - 1)^2 + (2\zeta_i \beta_{ik})^2]^{-1} \tag{8}$$

and $\beta_{ik} = f_i / \mathrm{f}_k$. Substituting (7) into the NLLF leads to a form whose dependence on the modal parameters is mathematically intractable. Obtaining the MPV of modal parameters by brute-force numerical optimization is prohibitive as the number of parameters grows with the number of measured dofs and the number of setups. In view of this, an alternative but equivalent form of the NLLF has been derived which allows efficient computation

$$L(\boldsymbol{\theta}) = -(\ln 2)\sum_{i=1}^{n_s} n_i N_{fi} + \sum_{i=1}^{n_s}(n_i - 1)N_{fi}\ln S_{ei} + \sum_{i=1}^{n_s}\sum_{k}\ln(S_i D_{ik}\left\|\mathbf{L}_i\boldsymbol{\varphi}\right\|^2 + S_{ei}) + \sum_{i=1}^{n_s} S_{ei}^{-1} d_i - \boldsymbol{\varphi}^T\mathbf{A}(\boldsymbol{\varphi})\boldsymbol{\varphi} \tag{9}$$

where N_{fi} is the number of FFT ordinates in the selected frequency band in Setup i; and

$$\mathbf{A}(\boldsymbol{\varphi}) = \sum_{i=1}^{n_s} S_{ei}^{-1}\sum_{k}(\left\|\mathbf{L}_i\boldsymbol{\varphi}\right\|^2 + S_{ei}/S_i D_{ik})^{-1}\mathbf{L}_i^T\mathbf{D}_{ik}\mathbf{L}_i \in R^{n\times n} \tag{10}$$

$$\mathbf{D}_{ik} = \mathrm{Re}\,\mathcal{F}_{ik}\,\mathrm{Re}\,\mathcal{F}_{ik}^{\,T} + \mathrm{Im}\,\mathcal{F}_{ik}\,\mathrm{Im}\,\mathcal{F}_{ik}^{\,T} \in R^{n_i\times n_i} \tag{11}$$

$$d_i = \sum_{k}(\mathrm{Re}\,\mathcal{F}_{ik}^{\,T}\,\mathrm{Re}\,\mathcal{F}_{ik} + \mathrm{Im}\,\mathcal{F}_{ik}^{\,T}\,\mathrm{Im}\,\mathcal{F}_{ik}) \tag{12}$$

Based on (9), partial analytical solutions of the MPV of modal parameters have been derived, leading to a fast iterative algorithm that can be practically implemented even for a large number of dofs and setups. For details, please refer to Zhang (2011) and Au and Zhang (2012).

3. POSTERIOR UNCERTAINTY

The posterior covariance matrix of modal parameters can be obtained as the inverse of the Hessian of the NLLF. The basic computational issues associated with evaluating the posterior covariance matrix arise from the norm constraint of the mode shapes. When evaluating the Hessian of the NLLF, one simple strategy to correctly reflect the constraint is to write the mode shape explicitly in normalized form. That is, let

$$\overline{\boldsymbol{\varphi}} = \left\|\boldsymbol{\varphi}\right\|^{-1}\boldsymbol{\varphi} \tag{13}$$

be the mode shape that is normalized to have unit norm, i.e., $\left\|\overline{\boldsymbol{\varphi}}\right\| = 1$ regardless of $\boldsymbol{\varphi}$. For the determination of Hessian, the mode shape $\boldsymbol{\varphi}$ in the expression of the NLLF in (9) should be replaced by $\overline{\boldsymbol{\varphi}}$ so that the NLLF, as shown in the following equation, can be differentiated with respect to the free parameters in $\boldsymbol{\varphi}$ without any constraint.

$$L(\boldsymbol{\theta}) = -(\ln 2)\sum_{i=1}^{n_s} n_i N_{fi} + \sum_{i=1}^{n_s}(n_i - 1)N_{fi}\ln S_{ei} + \sum_{i=1}^{n_s}\sum_{k}\ln(S_i D_{ik}\frac{\left\|\mathbf{L}_i\boldsymbol{\varphi}\right\|^2}{\boldsymbol{\varphi}^T\boldsymbol{\varphi}} + S_{ei}) + \sum_{i=1}^{n_s} S_{ei}^{-1} d_i - \frac{\boldsymbol{\varphi}^T\mathbf{A}(\boldsymbol{\varphi}/\left\|\boldsymbol{\varphi}\right\|)\boldsymbol{\varphi}}{\boldsymbol{\varphi}^T\boldsymbol{\varphi}} \tag{14}$$

The resulting NLLF will be invariant to the scaling of $\boldsymbol{\varphi}$. Correspondingly the Hessian of the NLLF will be singular along the directions $\boldsymbol{\varphi}$. It will thus have one zero eigenvalue

along the eigen-direction $\boldsymbol{\varphi}$ and is therefore not invertible. However, it can be reasoned that this singularity is immaterial to the evaluation of the posterior covariance matrix, because the mode shape uncertainty is by definition orthogonal to such direction. Let $\{\lambda_i : i = 1,...,n_\theta\}$ and $\{\mathbf{w}_i \in R^{n_\theta} : i = 1,...,n_\theta\}$ be respectively the eigenvalues (in ascending order) and eigenvectors of the Hessian matrix of the NLLF at the MPV, where $n_\theta = n + 4n_s$ is the number of modal parameters. Then the Hessian has the eigenvector representation

$$\mathbf{H}_L = \sum_{i=1}^{n_\theta} \lambda_i \mathbf{w}_i \mathbf{w}_i^T = \sum_{i=2}^{n_\theta} \lambda_i \mathbf{w}_i \mathbf{w}_i^T \tag{15}$$

since $\lambda_1 = 0$. Ignoring the singular direction, the posterior covariance matrix as the inverse of $\mathbf{H}_L$ is evaluated as

$$\mathbf{C} = \sum_{i=2}^{n_\theta} \lambda_i^{-1} \mathbf{w}_i \mathbf{w}_i^T \tag{16}$$

In this subsection we present the second derivatives of the NLLF, which allows its Hessian and hence the posterior covariance of the modal parameters to be evaluated accurately and efficiently without resorting to finite difference. The derivatives are obtained by direct differentiation of (14). The results are presented in terms of two main quantities, a_{ik} and b_{ik} in (19) and (20), respectively. For notational simplicity we use a superscripted symbol to denote derivatives with respect to that variable.

The second derivative of L with respect to the natural frequency in Setup i, f_i $(i = 1,...,n_s)$, is given by

$$L^{(f_i f_i)} = \sum_k (\ln b_{ik})^{(f_i f_i)} - S_{ei}^{-1} (\sum_k a_{ik}^{(f_i f_i)} p_{ik}) \tag{17}$$

where

$$p_{ik} = \frac{\boldsymbol{\varphi}^T \mathbf{L}_i^T \mathbf{D}_{ik} \mathbf{L}_i \boldsymbol{\varphi}}{\boldsymbol{\varphi}^T \boldsymbol{\varphi}} \tag{18}$$

depends only on the data in Setup i (through $\mathbf{D}_{ik}$) and the global mode shape $\boldsymbol{\varphi}$; and

$$a_{ik} = (\frac{\left\|\mathbf{L}_i \boldsymbol{\varphi}\right\|^2}{\boldsymbol{\varphi}^T \boldsymbol{\varphi}} + S_{ei} / S_i D_{ik})^{-1} \tag{19}$$

$$b_{ik} = S_i D_{ik} \frac{\left\|\mathbf{L}_i \boldsymbol{\varphi}\right\|^2}{\boldsymbol{\varphi}^T \boldsymbol{\varphi}} + S_{ei} \tag{20}$$

The derivatives of a_{ik} and $\ln b_{ik}$ will be omitted here. For details, please refer to Zhang et al (2014). The forms of the expressions of $L^{(\zeta_i \zeta_i)}$ and $L^{(S_i S_i)}$ are similar to $L^{(f_i f_i)}$ in (17).

The second derivative of L with respect to the PSD of prediction error in Setup i, $S_{ei}(i=1,...,n_s)$, is given by

$$L^{(S_{ei}S_{ei})} = -S_{ei}^{-2}[N_{fi}(n_i-1)] + \sum_k (\ln b_{ik})^{(S_{ei}S_{ei})} - S_{ei}^{-1}\sum_k a_{ik}^{(S_{ei}S_{ei})} p_{ik} + 2S_{ei}^{-2}\sum_k a_{ik}^{(S_{ei})} p_{ik} + 2S_{ei}^{-3}(d_i - \sum_k a_{ik} p_{ik}) \tag{21}$$

The second derivative of L with respect to the global mode shape $\boldsymbol{\varphi}$ is given by

$$\begin{aligned} L^{(\boldsymbol{\varphi}\boldsymbol{\varphi})} &= \sum_{i=1}^{n_s}\sum_k (\ln b_{ik})^{(\boldsymbol{\varphi}\boldsymbol{\varphi})} \\ &- 2S_{ei}^{-1}\sum_{i=1}^{n_s}\sum_k a_{ik}\left[\frac{\mathbf{L}_i^T\mathbf{D}_{ik}\mathbf{L}_i}{\boldsymbol{\varphi}^T\boldsymbol{\varphi}} - \frac{2\boldsymbol{\varphi}\boldsymbol{\varphi}^T\mathbf{L}_i^T\mathbf{D}_{ik}\mathbf{L}_i}{(\boldsymbol{\varphi}^T\boldsymbol{\varphi})^2} + \frac{4\boldsymbol{\varphi}\boldsymbol{\varphi}^T(\boldsymbol{\varphi}^T\mathbf{L}_i^T\mathbf{D}_{ik}\mathbf{L}_i\boldsymbol{\varphi})}{(\boldsymbol{\varphi}^T\boldsymbol{\varphi})^3} - \frac{2\mathbf{L}_i^T\mathbf{D}_{ik}\mathbf{L}_i\boldsymbol{\varphi}\boldsymbol{\varphi}^T}{(\boldsymbol{\varphi}^T\boldsymbol{\varphi})^2} - \frac{\boldsymbol{\varphi}^T\mathbf{L}_i^T\mathbf{D}_{ik}\mathbf{L}_i\boldsymbol{\varphi}\mathbf{I}_n}{(\boldsymbol{\varphi}^T\boldsymbol{\varphi})^2}\right] \\ &- 2S_{ei}^{-1}\sum_{i=1}^{n_s}\sum_k (a_{ik}^{(\boldsymbol{\varphi})})^T\left[\frac{\boldsymbol{\varphi}^T\mathbf{L}_i^T\mathbf{D}_{ik}\mathbf{L}_i}{\boldsymbol{\varphi}^T\boldsymbol{\varphi}} - \frac{\boldsymbol{\varphi}^T(\boldsymbol{\varphi}^T\mathbf{L}_i^T\mathbf{D}_{ik}\mathbf{L}_i\boldsymbol{\varphi})}{(\boldsymbol{\varphi}^T\boldsymbol{\varphi})^2}\right] \\ &- 2S_{ei}^{-1}\sum_{i=1}^{n_s}\sum_k \left[\frac{\mathbf{L}_i^T\mathbf{D}_{ik}\mathbf{L}_i\boldsymbol{\varphi}}{\boldsymbol{\varphi}^T\boldsymbol{\varphi}} - \frac{(\boldsymbol{\varphi}^T\mathbf{L}_i^T\mathbf{D}_{ik}\mathbf{L}_i\boldsymbol{\varphi})\boldsymbol{\varphi}}{(\boldsymbol{\varphi}^T\boldsymbol{\varphi})^2}\right] a_{ik}^{(\boldsymbol{\varphi})} - S_{ei}^{-1}\sum_{i=1}^{n_s}\sum_k a_{ik}^{(\boldsymbol{\varphi}\boldsymbol{\varphi})} p_{ik} \end{aligned} \tag{22}$$

The cross derivative of L with respect to f_i and ζ_i is given by

$$L^{(f_i\zeta_i)} = \sum_k (\ln b_{ik})^{(f_i\zeta_i)} - S_{ei}^{-1}(\sum_k a_{ik}^{(f_i\zeta_i)} p_{ik}) \tag{23}$$

Similarly, the cross derivative of L with respect to f_i and S_i is given by

$$L^{(f_iS_i)} = \sum_k (\ln b_{ik})^{(f_iS_i)} - S_{ei}^{-1}(\sum_k a_{ik}^{(f_iS_i)} p_{ik}) \tag{24}$$

The form of the expression of $L^{(\zeta_iS_i)}$ is similar to $L^{(f_iS_i)}$.

The cross derivative of L with respect to f_i and S_{ei} is given by

$$L^{(f_iS_{ei})} = \sum_k (\ln b_{ik})^{(f_iS_{ei})} + S_{ei}^{-2}(\sum_k a_{ik}^{(f_i)} p_{ik}) - S_{ei}^{-1}(\sum_k a_{ik}^{(f_iS_{ei})} p_{ik}) \tag{25}$$

The forms of the expression of $L^{(\zeta_iS_{ei})}$ and $L^{(S_iS_{ei})}$ are similar to $L^{(f_iS_{ei})}$.

The cross derivative of L with respect to f_i and $\boldsymbol{\varphi}$ is given by

$$L^{(f_i\boldsymbol{\varphi})} = \sum_k (\ln b_{ik})^{(f_i\boldsymbol{\varphi})} - S_{ei}^{-1}(\sum_k a_{ik}^{(f_i\boldsymbol{\varphi})} p_{ik})$$
$$- 2S_{ei}^{-1}\sum_k a_{ik}^{(f_i)}(\frac{\boldsymbol{\varphi}^T\mathbf{L}_i^T\mathbf{D}_{ik}\mathbf{L}_i}{\boldsymbol{\varphi}^T\boldsymbol{\varphi}} - \frac{\boldsymbol{\varphi}^T\mathbf{L}_i^T\mathbf{D}_{ik}\mathbf{L}_i\boldsymbol{\varphi}\boldsymbol{\varphi}^T}{(\boldsymbol{\varphi}^T\boldsymbol{\varphi})^2}) \tag{26}$$

The forms of the expression of $L^{(\zeta_i\boldsymbol{\varphi})}$ and $L^{(S_i\boldsymbol{\varphi})}$ are similar to $L^{(f_i\boldsymbol{\varphi})}$.

The cross derivative of L with respect to S_{ei} and $\boldsymbol{\varphi}$ is given by

$$L^{(S_{ei}\boldsymbol{\varphi})} = \sum_k (\ln b_{ik})^{(S_{ei}\boldsymbol{\varphi})} - S_{ei}^{-1}[\sum_k a_{ik}^{(S_{ei}\boldsymbol{\varphi})} p_{ik} + 2\sum_k a_{ik}^{(S_{ei})}(\frac{\boldsymbol{\varphi}^T\mathbf{L}_i^T\mathbf{D}_{ik}\mathbf{L}_i}{\boldsymbol{\varphi}^T\boldsymbol{\varphi}} - \frac{\boldsymbol{\varphi}^T\mathbf{L}_i^T\mathbf{D}_{ik}\mathbf{L}_i\boldsymbol{\varphi}\boldsymbol{\varphi}^T}{(\boldsymbol{\varphi}^T\boldsymbol{\varphi})^2})]$$
$$+ S_{ei}^{-2}[\sum_k a_{ik}^{(\boldsymbol{\varphi})} p_{ik} + 2\sum_k a_{ik}(\frac{\boldsymbol{\varphi}^T\mathbf{L}_i^T\mathbf{D}_{ik}\mathbf{L}_i}{\boldsymbol{\varphi}^T\boldsymbol{\varphi}} - \frac{\boldsymbol{\varphi}^T\mathbf{L}_i^T\mathbf{D}_{ik}\mathbf{L}_i\boldsymbol{\varphi}\boldsymbol{\varphi}^T}{(\boldsymbol{\varphi}^T\boldsymbol{\varphi})^2})] \tag{27}$$

By the following equations, the Hessian matrix can be determined and so the covariance matrix can be obtained according to (16). For the detail, please refer to Zhang et al (2014).

4. ILLUSTRATIVE APPLICATIONS

A pedestrian bridge is presented to illustrate the proposed method and its practical applications. A detailed mode shape is identified using a large number of setups with only four triaxial sensors. This example demonstrates the real challenges in assembling mode shape in practical situations. The pedestrian bridge named Footbridge NF276 (Highways Department, HKSAR) spans across the Tolo Harbor in the Eastern New Territories, Hong Kong. The bridge has a width of 12 m and a total length of 220m. It is supported continuously on six piers spacing 30m apart. Figure 1 shows the plan view of the bridge and the locations to be measured. The picture in Figure 2 was taken from the lower left of Figure 1. On either side of the bridge there are 37 locations, each to be measured triaxially, giving $37\times 2\times 3 = 222$ dofs. On two sides along the bridge there are handrails made of identical frames, each measuring 1.5m long. Advantage was taken of this to define the sensor locations to space at every four frames of the handrails. The resulting spacing is about 6 m. For the ease of implementation, the two roving sensors were placed at opposite positions across the width of the bridge. The reference locations were chosen near the mid-span and quarter span, at Locations 119 and 214, respectively.

Four triaxial force-balanced accelerometers, each pairing with a data recorder were available for the test. The overall channel noise is about 0.5 $\mu g/\sqrt{Hz}$. The four recorders were synchronized with GPS clock. Acceleration data was recorded at a sampling rate of 200Hz. Five minutes of ambient acceleration data was collected in each setup and used for analysis. Thirty-seven setups were planned to cover all the 74 locations. The setups were numbered according to their position on the bridge. The transition between setups, including moving, orienting and leveling sensors, could typically be finished in five minutes.

Each test thus required ten minutes. Including initial setup and calibration, the whole series of tests took about seven hours (from 0935 hrs to 1620 hrs).

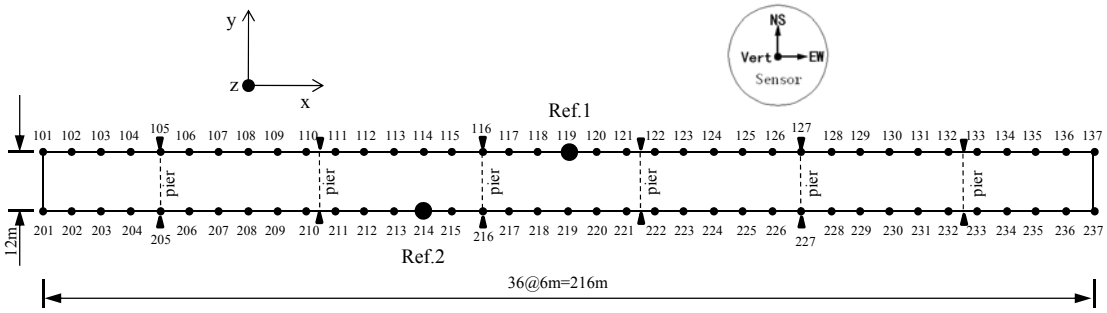

Figure 1 Setup locations, Footbridge NF276

Figure 2 Overall view of Footbridge NF276

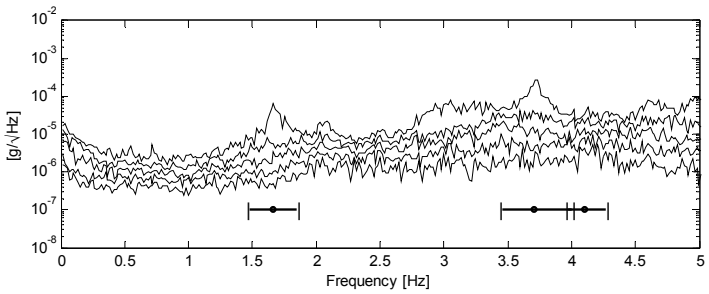

Figure 3 Root SV spectrum (averaged for viewing modes only), Setup 1, Footbridge NF276

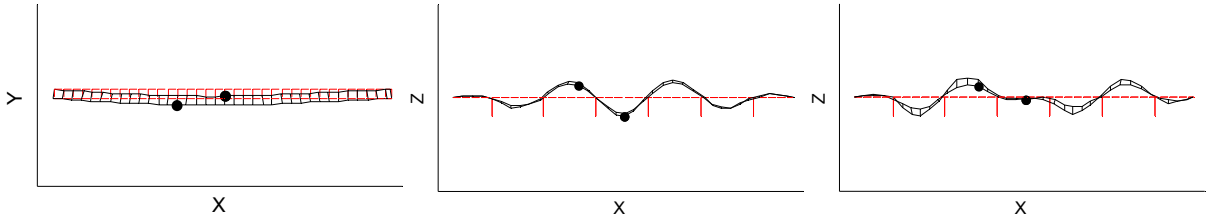

(a) Mode 1 (1.67Hz) (b) Mode 2 (3.76Hz) (c) Mode 3 (4.16Hz)

Figure 4 Identified mode shapes of Footbridge NF276

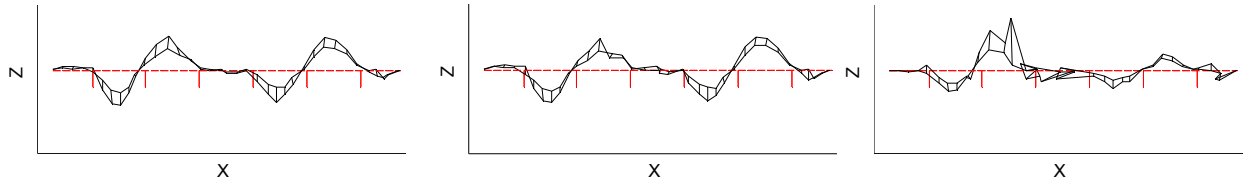

(a) Setup 20 (Good) (b) Setup 3 (Acceptable) (c) Setup 21 (Poor)

Figure 5 Assembled mode shape of Mode 3 by taking different setup as reference using conventional scaling method

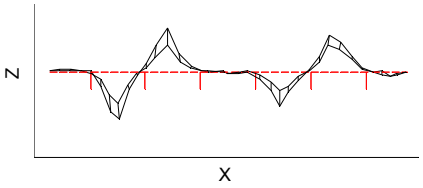

Figure 6 Assembled mode shape of Mode 3 by global least square method

Figure 3 shows the root SV spectra calculated using the data in Setup 1. It is used for locating the initial guess of the natural frequency and the frequency band for modal identification, focusing on the modes indicated. The modes are picked as suggested by their peaks. The frequency band should cover sufficiently the peak of the mode. It need not be excessively wide, however, since the tail contains little information and it increases the risk of modeling error. Figure 4 shows the most probable mode shapes of Mode 1 to Mode 3, respectively. The dashed and solid lines denote the undeformed and deformed shape, respectively. The first mode is flexural in the transverse direction. Mode 2 involves symmetric vertical bending. Mode 3 is also a vertical bending mode but it is asymmetric.

We next compare the results produced by the proposed method with those by two existing mode shape assembly methods, namely, a conventional scaling method based on a reference setup; and a recently developed global least square method (Au, 2011a). In the conventional scaling method, a reference setup is first selected. The second method is the global least square method determines the best fit global mode shape as the one that minimizes the global measure-of-fit function accounting for the discrepancy between the theoretical and the individually identified mode shapes in all setups. For the first two modes, the global (assembled) mode shape produced by the proposed, conventional method and global least square method are practically the same, with an MAC over 99%. Here, the quality of the assembled results is insensitive to the method used because the two modes are well-identified in all setups and their mode shape values at the reference dofs (not shown here) agree very well among setups.

Mode 3, however, presents the real challenge for mode shape assembly. Using the conventional scaling method, the mode shape has been assembled using different setups as reference. By visual inspection the assembled mode shapes are classified as ‘good’, ‘acceptable’ or ‘poor’. Figure 5(a), (b) and (c) show the assembled mode shapes when the reference setup is Setup 20, 3 and 21, respectively. These results cover the typical ones, representative of good, acceptable and poor quality. Setup 3 is not considered a good

reference because the resulting mode shape has a slope discontinuity at the third span from the left, which is not physically plausible. To provide the overall picture, Setups 6-14, 20, 22-32 as reference are considered 'good'; Setups 1-4, 15-16, 33, 35-37 are considered 'acceptable'; Setups 5, 17-19, 21, 34 are considered 'poor'. Roughly speaking, setups with roving sensors at the second or third span from either the left or right side are good reference. This appears intuitive because the mode shape values at these spans are significantly nonzero. Presumably, these setups help provide modal information for assembly, which is critical for Mode 3 because one of the reference sensors (Ref. 1) is near the nodal region of the mode shape. At any rate, the decision on choosing a good reference setup depends on the mode in question. Nevertheless, the mode shape is not known before it is calculated.

Figure 6 shows the mode shape assembled by the global least square method. It is similar to that produced by the proposed method but there are some important differences. Taking x-z view, the mode shape has a discontinuity in slope near the troughs and crests. In the absence of Figure 4(c), it would be difficult to ascertain whether such discontinuity reflects the real structural behavior (e.g., a hinge) or merely computational artifacts. The mode shape in Figure 4 (c) is physically more plausible. Note that the MAC is 95% between the global mode shape determined by the proposed and the global least square method. This value only indicates the overall discrepancy but contains no information regarding the local features.

Another focus of the example is to investigate the difference in posterior uncertainty between analyzing the data in different setups separately (as is conventionally done) and together (as proposed in this work). In particular, the posterior coefficient of variation (c.o.v.) of the modal parameters in a particular setup, say, Setup i, can be calculated using its own set of data only. On the other hand, in the context of the proposed Bayesian framework for multiple setups, these quantities can also be calculated by incorporating the data in all setups together. It is then of interest to see whether these two sets of results are similar and the circumstances where they are not. Throughout the examples, Method I refers to analyzing each setup individually (Au 2011b; Zhang and Au 2013; Au 2012a; Au 2012b); Method II refers to analyzing the data in all setups together according to the proposed framework.

Figure 7 to Figure 9 show the identified natural frequencies, and damping ratios corresponding to different setups, where each parameter is shown with a dot at the MPV and an error bar covering +/- 2 posterior standard deviations. The dashed lines denote the exact values of the modal parameters that generated the data. The results from Method I and Method II are shown with $<-\circ->$ (blue line) and $|-\bullet-|$ (black line), respectively. The results in different setups are shown chronologically and therefore some continuity (though in a statistical sense) in the results from one setup to the next should be expected if identification quality is good. It is clear from the figures that the identified modal parameters in terms of their posterior distribution vary from one setup to another. One possible reason is temperature effect, recognizing that the field test was performed from the morning to the afternoon.

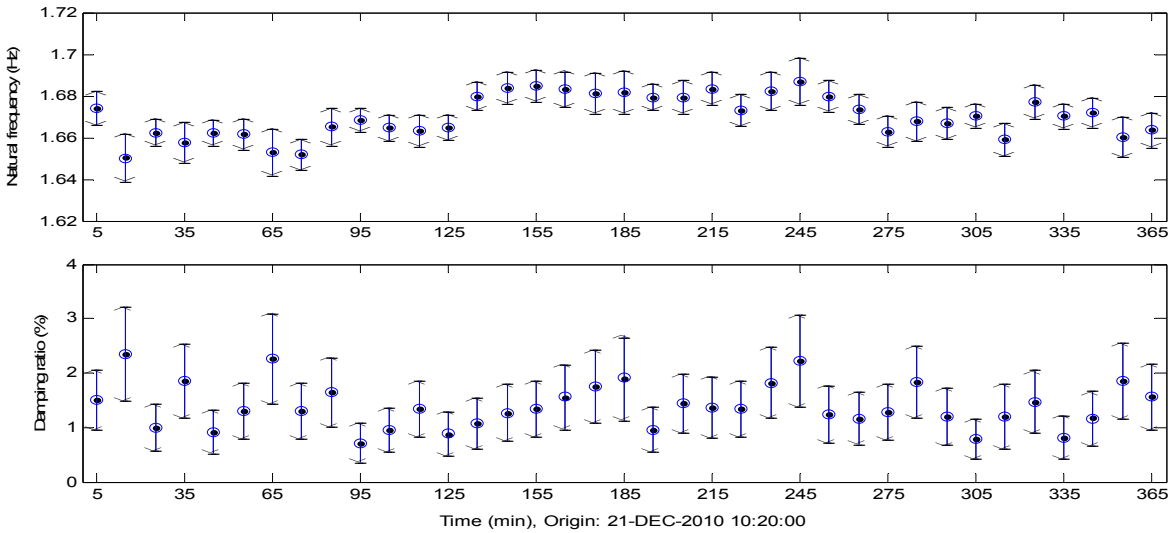

Figure 7 Identification result (±2standard derivation error bar) of natural frequency, damping ratio and modal force PSD, Mode 1; Method I (setup analyzed individually): <–○–> (blue line), Method II (setup analyzed together, proposed): |–●–| (black line).

In this context, the results by Method I and II generally agree for Mode 1 (Figure 7) and Mode 2 (Figure 8). These are the modes where modeling error is not significant and the s/n ratio is good, as evidenced in Figure 3 where their resonance peaks reasonably resembles the dynamic amplification factor. Other possibilities do exist where the results of Method I and II do not agree, as can be seen in Mode 3 (Figure 9). This mode is suspected of higher modeling error and lower s/n ratio, as evidenced from Figure 3 where their resonance peaks deviate significantly from what is usually expected of the variation of the dynamic amplification factor. It is possible for Method I and II to differ in both the MPV (dot and circle) and the posterior standard deviation (error bars).

A significant difference is observed in the posterior distribution (error bar) in some setups, which are highlighted in Figure 9. In this case there is little or no overlap between the error bars of Method I and II, indicating a significant difference in the identification conclusions. Although both Method I and Method II are Bayesian, Method I has not made full use of the data because it has not taken into account of the fact that the different setups have some reference dofs measured in common. This alone is sufficient to show preference on the results of Method II over Method I. Nevertheless it is also substantiated by the highlighted results. The posterior distribution implied from Method II generally has better continuity with respect to the setups which are arranged chronologically, while that of Method I has occasional discontinuities that are physically less plausible. The highlighted setups in Figure 9 typically have small s/n ratios and potentially significant modeling errors. When their data are analyzed individually (Method I) the identification results of the mode shape values at the reference dofs do not agree with other setups.

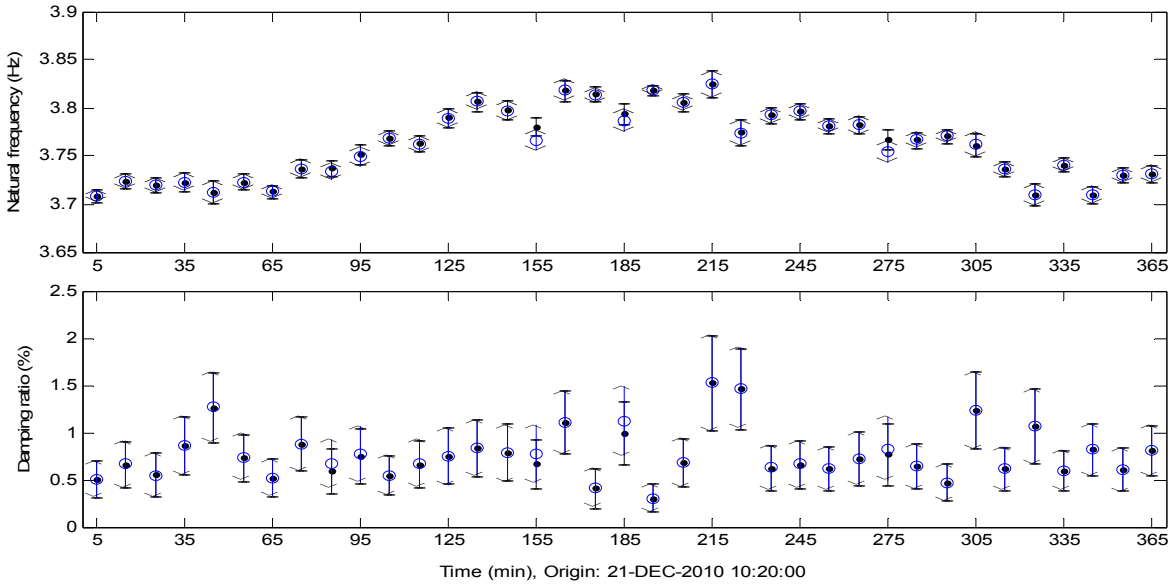

Figure 8 Identification result (±2standard derivation error bar) of natural frequency, damping ratio and modal force PSD, Mode 2; Method I (setup analyzed individually): <–○–> (blue line), Method II (setup analyzed together, proposed): |–●–| (black line).

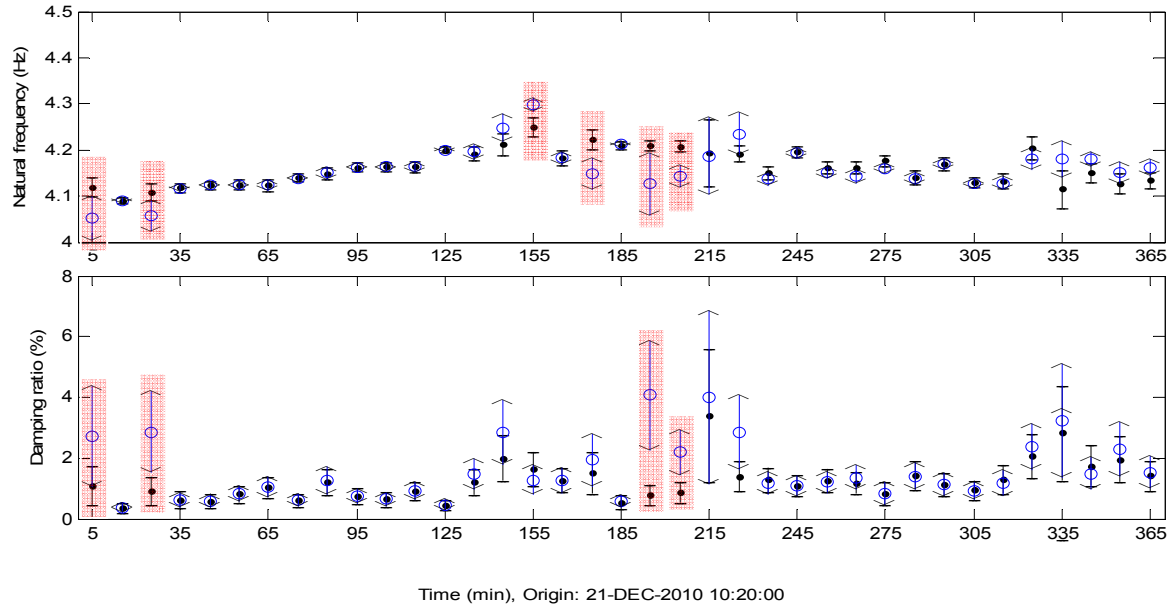

Figure 9 Identification result (±2standard derivation error bar) of natural frequency, damping ratio and modal force PSD, Mode 3; Method I (setup analyzed individually): <–○–> (blue line), Method II (setup analyzed together, proposed): |–●–| (black line). Setups where the MPV of Methods I & II differ significantly are shaded in red.

For Mode 3, if the data in different setups are not used together for identification, there is fundamentally no other information that can give a reliable conclusion on the mode shape values at the reference dofs. Moreover, these unreasonable mode shape values are associated with low quality of other modal properties such as natural frequency and damping ratio. The results demonstrate that, by incorporating the data in different setups together, it is possible for setups with good quality data to improve the identification results of setups with low quality data, through the reference dofs. Of course, this is only an intuitive statement; the actual mechanism by which this is done is through the likelihood function and is highly non-trivial.

5. CONCLUSIONS

This paper has presented a fast Bayesian FFT method for modal identification capable of incorporating information from multiple setups together with the analytical posterior uncertainty of the modal parameters in terms of their covariance matrix. A fast iterative procedure has been developed to obtain the most probable parameters. The method also makes it possible to perform the quantitative assessment of the accuracy of the identified modal parameters incorporating multiple setups and provides important information for the subsequent model updating, damage detection and structural health monitoring, etc.

An illustrative application has been presented, which demonstrate the practicability of the method. With field data it shows that the assembled mode shape is insensitive to the method used if the mode shapes in individual setups are well-identified, in the sense that they agree well at the reference dofs. Challenging situations do exist, when significant disagreement appears in some setups. In this case, for the conventional scaling method the choice of the reference setup depends on the mode shape but it is not always trivial a priori. For the global least square method, the result is more robust, but the poor quality of the identified mode shapes in some setups may smear into those that were originally well-identified.

The proposed Bayesian approach is found to produce a global mode shape that is physically plausible despite the significant disagreement present in some setups. Through the investigation of the difference between Method I (analyzing the data in different setups separately) and Method II (analyzing different setups together), it is concluded that for the modes where modeling error is not significant and the signal to noise (s/n) ratio is good, it does not make significant difference in the identification results whether the data in different setups are analyzed individually or together. For the modes that are suspected of higher modeling error and lower s/n ratio, it is possible for Method I and II to differ in both the MPV and the posterior standard deviation. For some typical setups, the modal parameters and their associated posterior uncertainty obtained by Method I have some discontinuities compared with other common setups, while proposed method (Method II) can still give reasonable results.

ACKNOWLEDGMENTS

This paper is funded by a start funding from Research Institute of Structural Engineering and Disaster Reduction, Tongji University (Project No. 0270128002) and partially by the Hong Kong Research Grant Council through General Research Fund (CityU 110012 (GRF 9041758)) .The financial support is gratefully acknowledged.

REFERENCES

Au, S.K. (2011a). "Assembling mode shapes by least squares", *Mechanical Systems and Signal Processing*, Vol. **25**(1), 163-179.

Au, S.K. (2011b). "Fast Bayesian FFT method for ambient modal identification with separated modes", *Journal of Engineering Mechanics,* ASCE, Vol. **137**(3), 214-226.

Au, S.K. (2012a). "Fast Bayesian ambient modal identification in the frequency domain, part I: posterior most probable value", *Mechanical Systems and Signal Processing*, Vol. **26**, 60-75.

Au, S.K. (2012b). "Fast Bayesian ambient modal identification in the frequency domain, part II: posterior uncertainty". *Mechanical Systems and Signal Processing*, Vol. **26**, 76-90.

Au, S.K. and Zhang, F.L. (2012). "Ambient modal identification of a primary-secondary structure by Fast Bayesian FFT method". *Mechanical Systems and Signal Processing,* Vol. **28**, 280–296.

Brownjohn, J. M. W. (2003). "Ambient vibration studies for system identification of tall buildings", *Earthquake Engineering and Structural Dynamics*, Vol. **32**, 71-95.

Peeters, B. and De Roeck, G. (2001). "One-year monitoring of the Z24-Bridge: environmental effects versus damage events", *Earthquake Engineering and Structural Dynamics*, Vol. **30**, 149-171.

Zhang, F.L. and Au, S.K. (2011). "Ambient modal identification of a fan-shaped slab using Fast Bayesian FFT method", *8th International Conference on Structure Dynamics (EURODYN 2011)*, Leuven, Belgium, 4-6 July.

Zhang, F.L. (2011), *Bayesian Ambient Modal Identification with Multiple Setups*, PhD Thesis, Department of Civil and Architectural Engineering, City University of Hong Kong.

Zhang, F.L. and Au, S.K. (2013), "Erratum for Fast Bayesian FFT method for ambient modal identification with separated modes by Siu-Kui Au". *Journal of Engineering Mechanics, ASCE*; Vol. **139** (4), 545-545.

Zhang, F.L., Au, S.K. and Lam, H.F. (2014). "Assessing uncertainty in operational modal analysis incorporating multiple setups using a Bayesian approach." *Structural Control and Health Monitoring*. DOI: 10.1002/stc.1679. In print.